Structural and electronic properties of a wide-gap quaternary alloy: $Zn_xMg_{1-x}S_ySe_{1-y}$

A.M. Saitta,[1,a,*] S. de Gironcoli,[1*] and S. Baroni[1,2*]
[1] *INFM – Istituto Nazionale per la Fisica della Materia and*
SISSA – Scuola Internazionale Superiore di Studi Avanzati, Via Beirut 2-4, I-34014 Trieste, Italy
[2] *CECAM – Centre Européen de Calcul Atomique et Moléculaire, ENSL, 46 Allée d'Italie, 69364 Lyon Cedex 07, France*
(February 7, 2008)

The structural properties of the $Zn_xMg_{1-x}S_ySe_{1-y}$ solid solutions are determined by a combination of the *computational alchemy* and the *cluster expansion* methods with Monte Carlo simulations. We determine the phase diagram of the alloy and show that the homogeneous phase is characterized by a large amount of short-range order occurring among first-nearest neighbors. Electronic-structure calculations performed using the *special quasi-random structures* approach indicate that the energy gap of the alloy is rather sensitive to this short-range order.

Wide gap semiconductors have recently attracted an enormous technological interest [1] both because of their potential use in devices capable of operating at high power level and high temperature, and because of the need for optical materials active in the blue-green spectral range. ZnSe-based technology will be used for operation in this spectral range provided that current device lifetime problems are overcome. One major goal of materials engineering for opto-electronic applications is the ability to tune *independently* the band gap, E_g—in order to obtain the desired optical properties—and the lattice parameter, a_0, of the material—in order to be able to grow it on a given substrate. Unfortunately, in most III-V and II-VI alloys, the additional degree of freedom provided by alloying both the cationic and the anionic sub-lattices cannot be effectively exploited because E_g and a_0 are roughly inversely proportional to one another for any values of the cationic and anionic compositions, (x, y). From this point of view, $Zn_xMg_{1-x}S_ySe_{1-y}$ alloys play a special role, in that the lattice parameter and optical gap can be varied fairly independently as functions of (x, y) [2].

In spite of this big interest, many technical difficulties still hinder a precise experimental characterization of these materials, so that their equilibrium structural and optical properties are basically unknown. In this Letter we report on the first application of state-of-the-art electronic-structure techniques to the determination of the structural and optical properties of a quaternary (double binary) semiconductor alloy at thermodynamic equilibrium, and present results in the specific case of $Zn_xMg_{1-x}S_ySe_{1-y}$. Even though MBE-grown materials are fabricated in highly non-equilibrium conditions, understanding their equilibrium properties is preliminary to any further investigations and provides the physical limits to the tunability of the alloy properties.

The first goal of this Letter is to determine the thermodynamic stability of the (Zn,Mg)(S,Se) solid solution with respect to segregation into its constituents and/or to the formation of ordered structures. Secondly, we will analyze how the fundamental gap depends on compositions and the role that short-range order plays in the electronic properties of this material.

The thermodynamic properties of $Zn_xMg_{1-x}S_ySe_{1-y}$ are studied by mapping the alloy onto a (double) lattice-gas model [3,4] that is solved by standard Monte Carlo techniques. To this end, an Ising-like variable, $\{\sigma_{\mathbf{R}s}\}$, is first attached to the s-th atom in the elementary cell located at $\mathbf{R}$, and it is assumed to take the values ± 1 according to the type of atom occupying that lattice site. The energy of the alloy is then expanded in terms of the σ's including terms up to three-spin interactions:

$$E\left(\{\sigma\}\right) = E_0 + \sum_{\mathbf{R}s} K_s \sigma_{\mathbf{R}s} + \frac{1}{2} \sum_{\substack{\mathbf{R}\mathbf{R}' \\ ss'}} J_{ss'}\left(\mathbf{R}-\mathbf{R}'\right) \sigma_{\mathbf{R}s}\sigma_{\mathbf{R}'s'} + \\ + \frac{1}{6} \sum_{\substack{\mathbf{R}\mathbf{R}'\mathbf{R}'' \\ ss's''}} L_{ss's''}\left(\mathbf{R}-\mathbf{R}'', \mathbf{R}'-\mathbf{R}''\right) \sigma_{\mathbf{R}s}\sigma_{\mathbf{R}'s'}\sigma_{\mathbf{R}''s''}. \qquad (1)$$

The validity of the truncation is then established *a posteriori*. The two- and three-body interaction constants, J and L, can in principle be obtained from both the *cluster expansion* (CE) [5] or *computational alchemy* (CA) [6] approaches. The explicit inclusion of local distortions from the ideal lattice positions—due to the different atomic sizes—renormalizes the two-body interaction, making it long-ranged [6] and hence hardly obtainable by the CE method. In principle, the three-body interactions, L, could also be computed within CA by making use of the so called *2n+1 theorem* [7]. Assuming that the L's are short-ranged, however, they are more conveniently obtained by the CE method. To this end, we first calculate the J's up to 9-th nearest neighbors from CA by using second-order density-functional perturbation theory [8]. We then assume that the only non-vanishing L's are those which connect atoms that are first- or, at most, second-nearest neighbors. Because of symmetry, there are only six such 3-body interaction constants. In the zincblende structure, there are two inequivalent triplets of second-nearest neighbors which differ according to whether or not they have a common first-nearest neighbor. We follow the common practice of neglecting such difference [5], and we keep 4 inequivalent 3-body interactions. In order to determine the latter, we have calculated the total

energies of a set of 28 pseudo-binary ordered structures by using self-consistent density-functional theory (DFT) within the local-density approximation (LDA) [8], and by allowing the lattice to relax until the forces acting on individual atoms vanish. We have then fitted the cubic term of Eq. (1) to the differences between the energies so calculated and the predictions of Eq. (1), when truncated to second order. The quality of the fit so obtained is finally checked against 39 additional quaternary structures. The resulting mean-square error is $\lesssim 0.8$ meV per atom pair, while the maximum error is 2.1 meV. Two- and three-body constants have been calculated for 5 and 3 volumes in the range $[V_{\rm ZnS}, V_{\rm MgSe}]$ respectively, and interpolated in-between.

Finite-temperature properties have been determined by lattice-gas Monte Carlo simulations, using supercells of 1024 atoms, at constant temperature, pressure, and chemical potentials. To this end, we attempt two different types of Monte Carlo moves: the reversal (flip) of each spin and a variation of the volume of the supercell. The trial move is then accepted with the Metropolis probability. Measures were taken over $\approx 10^3$ correlation times after thermal equilibrium was reached.

The free energy surface of the system is extracted from the determination of the compositions, x and y, as functions of the chemical potentials, μ_x and μ_y. The regions of *spinodal* (local) stability correspond to those concentrations for which the Hessian of the free energy with respect to the concentrations is positive definite. The thermodynamically stable concentrations (binodal regions), and thus the miscibility gaps, are determined with a generalization of the common-tangent Maxwell construction usually adopted for binary mixtures: the globally stable points are those which are locally stable and whose tangent planes do not intersect the free energy surface at any other points in the square of concentrations.

In Fig. 1 we display a cut of the phase diagram of the quaternary alloy at four different temperatures. At typical MBE growth temperatures (≈ 600 K) and above the alloy is predicted to be completely miscible. For $T = 550$ K (Fig. 1a), the disordered alloy is stable at all compositions but for a small island close to the $Zn_xMg_{1-x}Se$ pseudo-binary alloy centered around $x \approx 0.6$, whose computed critical temperature is of about 610 K. Decreasing the temperature (Fig. 1b) the size of the island increases and a forbidden region appears inside the square of compositions, close to the mid point $(x, y) = (\frac{1}{2}, \frac{1}{2})$. Cooling down to $T = 500$ K (Fig. 1c), the Mg-rich and the Zn-rich regions become separated by a "corridor" in which the disordered alloy is not locally stable. The concentrations of the phases in which the alloy segregates in the miscibility gap are given by the contact points of the tangent plane. Segregation may thus result in the separation into two or three phases, according to the number of contact points. In the present case, the critical temperatures of the pseudo-binary alloys with cationic

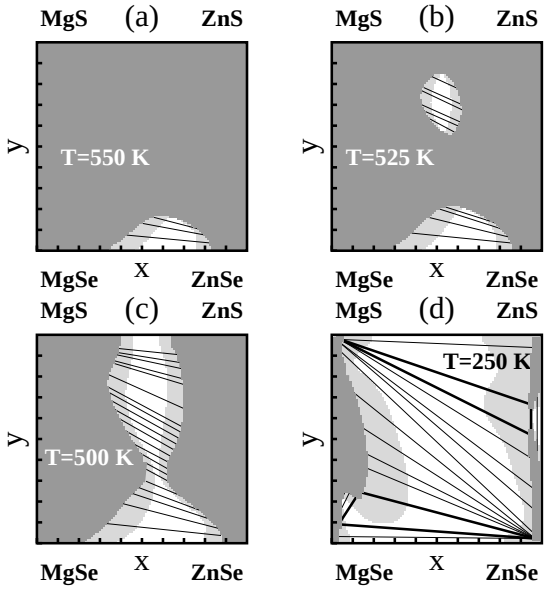

FIG. 1. Phase diagram of the alloy at four different temperatures. The dark gray (binodal) regions are thermodynamically stable. The light gray (spinodal) regions are only locally stable (metastable). The white regions are completely unstable. The segments inside the miscibility gap connect the stable phases identified by the common-tangent-plane construction (see text). In panels $a - c$ only separation into two phases occur. In panel d two cases where the products of separation are three distinct phases are indicated by thicker lines.

disorder, $Zn_xMg_{1-x}Se$ and $Zn_xMg_{1-x}S$, are much larger ($T_c = 613$ K and 511 K respectively) than those of the pseudo-binary alloys with anionic disorder, ZnS_ySe_{1-y} ($T_c = 254$ K) and MgS_ySe_{1-y} ($T_c = 243$ K); therefore, above room temperature the alloy segregates into two phases: a Zn-rich phase and a Mg-rich one. This behavior is due to the larger chemical difference between cations than between anions. At temperatures of the order of the anionic-alloy critical temperatures and below ($T \lesssim 250$ K), the tendency to segregation also involves the anionic sub-lattice, and separation into three phases may occur (Fig. 1d).

Our results show that in (Zn,Mg)(S,Se) the onset of segregation occurs at a critical temperature that is in the range of typical MBE growth temperatures, and thus much lower than in other II-VI quaternary alloys [9]. This result is in agreement with an analysis of experimental data [10], based on *delta-lattice-parameter* models [11], that locate T_c between 525 K and 625 K. According to the only experimental report [12] we are aware of, a forbidden region of compositions has been observed, at room temperature, inside the predicted miscibility gap.

The structural properties of the alloy can be extracted from our Monte Carlo simulations. The equilibrium lattice constant has a strong linear dependence upon compositions, thus following Vegard's law. Slight deviations

$$a_0(x,y) = a_{\rm MgSe} + Ax + By + Cxy + Dx^2 + Ey^2$$

	$a_{\rm MgSe}$	A	B	C	D	E
LDA	11.326	-0.789	-0.539	0.058	0.027	0.016
Corrected LDA	11.130	-0.443	-0.523	0.018	0.027	0.016

TABLE I. Quadratic fit coefficients for LDA (upper row) and "corrected" LDA (lower row) lattice constant of the alloy. The maximum error of the fit is of 0.05%, and the mean square error of 0.01%.

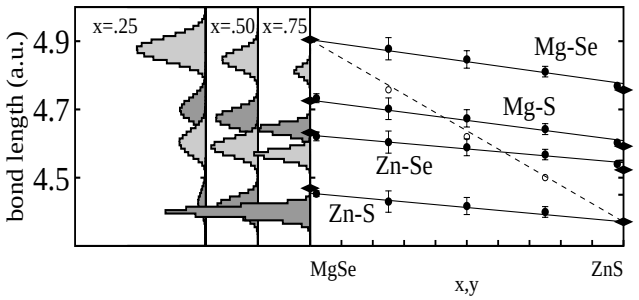

FIG. 2. Left panel: bond-length distributions along the ZnS − MgSe diagonal in the square of the compositions. Right panel: dependence of maxima of the peak upon the concentrations. Diamonds correspond to pure-material bond-lengths. Empty dots refer to the alloy lattice constant and the dashed line is a linear fit.

from this law are extracted by a fit of the lattice parameter of the alloy with a quadratic polynomial in x and y (see Table I). A direct comparison with experimental data may be done by correcting for the LDA error on the equilibrium lattice constants of the pure constituents of the alloy ($\pm 1 \div 2\%$), which is accounted for by a bilinear interpolation and added to the quadratic polynomial obtained above. The corrected coefficients of polynomial fit are also reported in Table I. The agreement with experimental data [2] is good in the Zn-rich region, especially in proximity of pure ZnSe, while it is apparently poor in the Mg-rich part of the square of the compositions, where however the instability of the system makes it very difficult to measure the concentrations with the same precision, and the experimental data are in fact very scarce.

As it is the case in other tetrahedrally bonded solid solutions, the Vegard's law does not result from a linear dependence of individual bond lengths upon compositions, but rather from a subtle topological compensation of bond lengths which stay in fact rather close to the values they would have in pure compounds [10]. This behavior is displayed in Fig. 2, where we show the bond lengths as obtained at T=800 K for the (Zn,Mg)(S,Se) alloy along the MgSe-ZnS diagonal of the square of concentrations (along the other diagonal the lattice parameter is almost constant and matched to that of GaAs). At any concentrations, while the lattice parameter of the alloy varies almost linearly by more than 12 %, the largest deviations between the bond lengths and their pure-compound values are smaller than 3%.

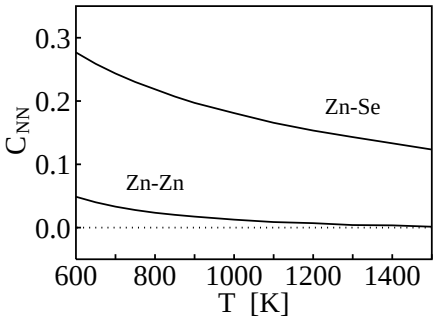

FIG. 3. First- and second-nearest-neighbors two-body correlations of the $Zn_{\frac{1}{2}}Mg_{\frac{1}{2}}S_{\frac{1}{2}}Se_{\frac{1}{2}}$ alloy as function of temperature.

The typical substrate on which such alloys are grown is GaAs, whose lattice constant is $a_0 = 10.68$ a.u., close to the equilibrium lattice parameters of ZnSe and MgS. Therefore, the technological relevant concentrations of the quaternary alloy are those located along the ZnSe-MgS diagonal of the square of the compositions. For these solid solutions, the Mg-Se and Zn-S bonds are consequently subject to a larger elastic strain with respect to the other bonds; the preferential formation of MgS and ZnSe clusters is thus expected to be energetically favored. In order to clarify this issue we have calculated the two-body correlations of the $Zn_{\frac{1}{2}}Mg_{\frac{1}{2}}S_{\frac{1}{2}}Se_{\frac{1}{2}}$ alloy at temperatures above the miscibility gap. The correlation function is defined as: $C_{ss'}(\mathbf{R}) = \langle \sigma_{s\mathbf{0}}\sigma_{s'\mathbf{R}}\rangle - \langle\sigma_s\rangle\langle\sigma_{s'}\rangle$. Therefore, $C_{ss'}(\mathbf{R}) = 0$ in the perfectly random alloy, $C_{ss'}(\mathbf{R}) > 0$ for ZnSe and MgS clusterizations, and $C_{ss'}(\mathbf{R}) < 0$ for ZnS and MgSe clusterizations. In correspondence of the first-nearest-neighbor shell, $C_{ss'}(\mathbf{R})$ has a very pronounced positive peak, thus indicating a strong tendency to form ZnSe and MgS clusters. This tendency is confirmed by the positive value of the cation-cation or anion-anion correlations in the second-nearest-neighbor shell, which are however weaker. Correlations practically die beyond the second shell of neighbors, and are therefore characteristic of a very pronounced short-range order (SRO). In Fig. 3 we display the value of the first- and second-shell correlation peaks for a range of temperatures above T_c. The nearest-neighbor correlation peak is still significantly large at very high temperature, thus indicating that short-range-order is present even close to the melting temperatures (above $T \approx 1700$ K): the system can never be described as a perfectly random alloy.

The second goal of this work is to study the influence of the structural properties of the alloy at the atomistic level on the electronic and optical properties. The band structure of a disordered material is strongly affected by its local environment that is poorly approximated by effective-medium approaches [13,14]. A detailed account of the microscopic structure of the alloy is even more important in the present case where SRO effects are expected to play a significant role. A "direct" DFT-LDA calculation should be in principle performed by using very large

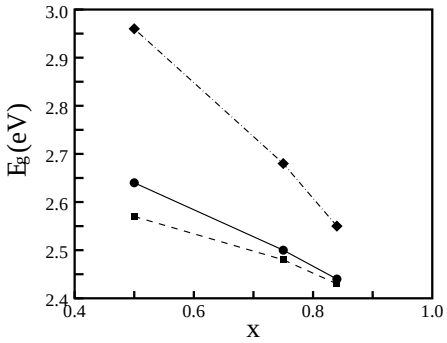

FIG. 4. Energy gap of the $(Zn, Mg)(S, Se)$ quaternary alloy lattice-matched to GaAs as function of the x composition (bottom scale) and y composition (top scale). The dot-dashed line refers to virtual crystal calculations, the dashed one to perfectly-random-alloy results, and the solid line to the short-range-ordered alloy band gaps.

supercells in order to cope with compositional disorder. Here we adopt the *special quasi-random structures* (SQS) approach [15], suitably generalized to account for SRO effects [16], double-sublattice disorder, and arbitrary compositions. We have considered three different concentrations along the line of lattice matching to GaAs, and chosen among the discrete set of compositions compatible with 64-atom SQS's and close to the ZnSe-rich region: $(x, y) = (\frac{1}{2}, \frac{1}{2}); (\frac{3}{4}, \frac{1}{8}); (\frac{27}{32}, 0)$. For these concentrations, SQS's have been obtained by a simulated-annealing procedure aimed at modeling the pair correlation functions at short range—as obtained from Monte Carlo simulations performed at $T = 550\ K$ and resulting in very faithful pair correlations up to fourth-nearest-neighbors. We have explicitly verified that the calculated electronic properties of the alloy are rather insensitive to correlations beyond this order of neighbors.

It is interesting to compare the results obtained using different levels of approximations to substitional disorder. In Fig. 4 we display the energy gap as a function of the cationic composition along the GaAs-matching line of the compositions plane, as obtained from calculations performed *i)* on the appropriate virtual crystal, *ii)* on supercells describing the perfectly random alloy, and *iii)* on SQS's that reproduce the SRO correlations as explained above. We see that virtual-crystal is a bad approximation of the real system, while the effects of SRO show up in a slight but non-negligible opening of the fundamental band gap. Our results, once bilinearly corrected for the DFT error in the pure materials, agree very well (within 40 meV), with freshly appeared experimental estimates [17]. An analysis of the momentum- and position-projected density of states shows that the fundamental gap is direct and occurs at the Γ point of the Brillouin zone for any concentrations. The top-valence band states are mainly Se states, while the bottom state of the conduction band is rather delocalized on the different atomic species and it is found to be the most sensitive to the occurrence of short-range-order.

We wish to thank A. Franciosi and S. Rubini for prompting our interest in this problem and for many fruitful discussions. A more complete account of this work can be found in the PhD thesis of one of us (AMS) which is available on the www [18]. This work has been done in part within the *Iniziativa Trasversale Calcolo Parallelo* of the INFM.

---

[a] Present address: *Center for Molecular Modeling, Dept. of Chemistry, University of Pennsylvania, 231 S 34th St, Philadelphia, PA 19104-6202*

* Electronic addresses: saitta@cmm.chem.upenn.edu, degironc@sissa.it, and baroni@sissa.it.

[1] *II-VI Blue/Green Light Emitters: Device Physics and Epitaxial Growth*, ed. by R. L. Gunshor and A. V. Nurmikko, Semiconductor and Semimetals **44**, Academic Press, (1997).

[2] H. Okuyama, K. Nakano, T. Miyajima, and K. Akimoto, Jpn. J. Appl. Phys. **30**, L1620 (1991); J. Cryst. Growth **117**, 139 (1992).

[3] D. de Fontaine, in *Solid State Physics*, edited by H. Ehrenreich, F. Seitz, and D. Turnbull (Academic, New York, 1979), **34**, 73.

[4] J. W. D. Connolly and A. R. Williams, Phys. Rev. B **27**, 5169 (1983).

[5] L. G. Ferreira, S.-H. Wei, and A. Zunger, Phys. Rev. B **40**, 3197 (1989); S.-H. Wei, L. G. Ferreira, and A. Zunger, Phys. Rev. B **41**, 8240 (1990).

[6] S. de Gironcoli, P. Giannozzi, and S. Baroni, Phys. Rev. Lett. **66**, 2116 (1991); N. Marzari, S. de Gironcoli, and S. Baroni, Phys. Rev. Lett. **72**, 4001 (1994).

[7] X. Gonze and J. P. Vigneron, Phys. Rev. B **39**, 13120 (1989).

[8] All our *ab-initio* calculations have been performed in the plane-wave pseudopotential scheme, adopting the non-linear core-correction description for Zn and Mg atoms, and choosing a kinetic-energy cutoff of 15 Ry and special **k**-points sampling of the Brillouin zone.

[9] D. W. Kisker, J. Cryst. Growth **98**, 127 (1989).

[10] T. Maruyama, *et al.*, J. Cryst. Growth **159**, 41 (1996).

[11] G. B. Stringfellow, J. Cryst. Growth **27**, 21 (1974); *ibid.* **65**, 454 (1983).

[12] B. J. Wu, *et al.*, Appl. Phys. Lett. **66**, 3462 (1995).

[13] L. Nordheim, Ann. Phys. (Leipzig) **9**, 607 (1931).

[14] P. Soven, Phys. Rev. **156**, 809 (1967); D. W. Taylor, *ibid.* **156**, 1017 (1967); U. Onodera and Y. Toyozawa, J. Phys. Soc. Jpn. **24**, 341 (1968); B. Velicky, S. Kirkpatrick, and H. Ehrenreich, Phys. Rev. **175**, 747 (1968).

[15] A. Zunger, S.-H. Wei, L. G. Ferreira, and J. E. Bernard, Phys. Rev. Lett. **65**, 353 (1990); S.-H. Wei, L. G. Ferreira, J. E. Bernard, and A. Zunger, Phys. Rev. B **42**, 9622 (1990); K. C. Hass, L. C. Davis, and A. Zunger, Phys. Rev. B **42**, 3757 (1990).

[16] K. A. Mäder and A. Zunger, Phys. Rev. B **51**, 10462 (1995).

[17] U. Lunz, *et al.*, Semicond. Sci. Technol. **12**, 970 (1997).

[18] A. M. Saitta, SISSA Ph. D. thesis, available at the URL: `http://www.sissa.it/cm/thesis/1997/`.